

## **Controlling G-quadruplex formation *via* lipid modification of oligonucleotide sequences**

Brune Vialet,<sup>† #</sup> Arnaud Gissot,<sup>† #</sup> Romain Delzor,<sup>†</sup> and Philippe Barthélémy<sup>†\*</sup>

<sup>†</sup> Inserm, U1212, CNRS 5320, Bordeaux, F-33076 France, Université de Bordeaux, F-33076, Bordeaux, France.

# These two authors contributed equally to the work.

***Supplementary information***

## List of acronyms:

G4: G-quadruplex

LON: Lipid OligoNucleotide

The Oligonucleotides used in this study are named after the presence (or absence) of the G4-prone DNA sequence:

### **x-OLIGONUCLEOTIDE<sup>y</sup>**

**x**: refers to the nature of the lipid either a mono octadecyl chain (**1**-) or dialkylated ketal (**k**-)

**y**: <sup>G4</sup>: G4-prone sequence or <sup>sc</sup>: scramble sequence

ex: **1-LON<sup>G4</sup>** : *n*-**C<sub>18</sub> H<sub>37</sub>** -5'- TTA GT **T GGG GT** T CAG TTG G -3' (G4-prone sequence in bold)

See Fig. 2 and S1 for the detailed list of oligonucleotides used.

## **Analytical Techniques:**

PAGE: PolyAcrylamide Gel Electrophoresis

CD: Circular Dichroism

DLS: Dynamic Light Scattering

## Experimental section:

### Automated DNA synthesis and purification of LONs.

LONs were synthesized using the phosphoramidite methodology on an automated Expedite 8909 DNA synthesizer at the  $\mu\text{mol}$  scale on 1000 Å primer support (loading: 30-100  $\mu\text{mol/g}$ , Link technologies, Synbase Control Pore Glass). Prior to use, the phosphoramidites **1** and **2** were dried over  $\text{P}_2\text{O}_5$  overnight and then dissolved in dry  $\text{CH}_2\text{Cl}_2/\text{CH}_3\text{CN}$  1/1 to a 0.1 M concentration (lipidic phosphoramidites do not dissolve in pure acetonitrile). N-benzylthiotetrazole was used for activation of the phosphoramidite prior to coupling. The phosphoramidite **1** and **2** were manually coupled at the 5' end of sequence on the solid support by passing (via syringes) the activator and the phosphoramidite solution (0.5 mL) back and forth several times for 10 min. Cleavage from the solid support and base deprotection was achieved using 1 mL of a saturated aqueous  $\text{NH}_4\text{OH}$  solution for 4 h at 55°C. The supernatant was collected and the CPG beads were washed 3 times with 200  $\mu\text{L}$  of milliQ water. The solutions were pooled and evaporated (speed vac). The crude LONs were dissolved in 0.5 mL of water and purified (except **k-LON<sup>G4</sup>**) on a semi-preparative  $\text{C}_4$ -reverse phase HPLC column (Macherey Nagel, Nucleosil, 5 $\mu\text{m}$ , 250mm), flow rate: 5 mL/min, using buffer A (0.1M triethylammonium acetate pH 7.1 /  $\text{CH}_3\text{CN}$  (95/5, V/V)) and buffer B 0.1M triethylammonium acetate pH 7.1 /  $\text{CH}_3\text{CN}$  (20/80, V/V), (see Figure S2 for details). The LONs eluted after 6,5 min. The LON containing fractions were pooled and evaporated to dryness and dissolved in autoclaved milliQ water. The (L)ONs were then dialyzed against a 10mM LiCl solution (not to favor G4 formation) followed by water. Yields were acceptable following this protocol (15-30% yield after purification of the crude material).

**k-LONs** were purified by preparative PAGE using conventional protocols with 20\*20\*0.2 cm 20% polyacrylamide gels at a limiting power of 15W. Importantly, we found that the quantity of **k-LON<sup>G4</sup>** that could be loaded on the gel did not exceed ca. 100 nmoles of crude material in ca. 300 $\mu\text{L}$  of loading sample. Higher amounts of crude LON led to substantial trailing of the LON band probably because of the formation of the micelles in that case even in the presence of heat + 7M urea in the running buffer. Using smaller quantities, the **k-LON<sup>G4</sup>** band is well defined (UV-shadow) and cut out directly with a clean scalpel. The gel slab was chopped into fine particles to elute the LON. We have been unsuccessful at eluting **k-LON<sup>G4</sup>** from the gel using different eluting buffers with additional heating (up to 90°C) and/or sonication and/or freeze and thaw protocols. Very small quantities of **k-LON<sup>G4</sup>** were systematically obtained for each of these tests.

We therefore developed an original electroelution protocol for the purification of these LONs (see Figure S3). In short, the electrical wire that was originally connected to the negative pole of the generator (black wire, Figure S3) was modified manually by wrapping a platinum wire around the naked copper wire. The latter was immersed in the eluting buffer contained in a plastic pipette that was chopped off at both edges to 1) facilitate pouring of the eluting buffer on top and 2) increase the cross section at the bottom to minimize resistance to the current flow. The bottom of the syringe was blocked by polymerizing 0.5mL of a 8% polyacrylamide solution (the bottom of the pipette being temporarily blocked by wrapping a parafilm foil around). After polymerization, the gel was prerun to remove any unpolymerized materials prior to loading the crushed acrylamide gel slab containing the LON (the TBE eluting buffer from the pipette was withdrawn beforehand for practical reasons). A dialysis tubing (with a cutoff of 2 kDa) was adapted and wrapped with a parafilm foil around the bottom of the pipette to recover the sample after electroelution. This allowed the dialysis tubing to be immersed in a large quantity of eluting buffer at the bottom in the electrophoresis tank. This step is crucial as a high power is required for elution (using a 50 mL spin tube instead in the absence of dialysis tubing led to a rapid increase in temperature of the solution followed by a short-circuit). The

elution was carried out with an electrical power of 7-10 W to allow enough heat dissipation in the gel to favor denaturation of the LONs. The LONs were finally dialyzed in a similar manner as described above for the other (L)ONs.

**Mass spectra** were recorded on a MALDI-ToF-ToF mass spectrometer (Ultraflex, Bruker Daltonics, Bremen, Germany). Best results were obtained in the linear mode with positive-ion detection. Mass spectra were acquired with an ion source voltage 1 of 25kV, an ion source voltage 2 of 23.5kV, a lens voltage of 6kV, by accumulating the ion signals from 1000 laser shots at constant laser fluence with a 100Hz laser. External mass calibration was achieved using a mixture of oligonucleotides dT<sub>12</sub>-dT<sub>18</sub> (Sigma). 1:1 mixture of samples of LONs (~20-50 $\mu$ M) and matrix was spotted on a MALDI target and air-dried before analysis. The performance of the following matrices was evaluated: 2,5-dihydroxybenzoic acid (DHB), 2,4,6-trihydroxy-acetophenone (THAP), 3-hydroxypicolinic acid (3-HPA) and 2,6-dihydroxyacetophenone (DHA). THAP at a concentration of 20 mg/mL in a 4:1 mixture of ethanol and 100mM aqueous ammonium citrate was shown to yield optimal mass spectral results (see Figure S1 for mass values).

**PAGE / agarose electrophoresis.** Electrophoresis experiments were performed according to standard procedures with 1% agarose gels. PAGE were carried out with 17% polyacrylamide gels (acrylamide-bis acrylamide 19:1, 40% w/v) and run with a 100V limiting tension for native PAGE experiments.

**Dynamic light scattering (DLS).** Particle size was determined using a Zetasizer 3000 HAS MALVERN. Experiments were realized with samples containing different concentration of LONs dissolved in deionized water or phosphate buffer. Measurements were performed at 25°C.

**Viscosizing or Taylor dispersion analyses** were recorded on a Viscosizer TD (Malvern Instruments Ltd., Malvern, UK equipped with a 254nm UV filter close to the  $\lambda_{\max}$  of oligonucleotides. Prior to analysis, the non-coated capillary has been prepared by injecting 1M NaOH during 30min at 3000mbar followed by 10min rinse with water at 3000mbar. The cellulose coated capillary has been prepared by injecting water during 30 min at 3000mbar. Internal Material (non-coated): fused silica, internal diameter: 75 $\mu$ m, outer diameter: 360 $\mu$ m, L1: 45cm, L2:85cm, Total Length: 130 cm. The samples were injected (pressure: 50mbar) analyzed at 25°C (Mobilization pressure: 140mbar). Taylorgrams were recorded and analyzed with the viscosizer TD software 2.01 with a one component fit. Washing: 1min of water between each sample, pressure: 3000mbar (Results shown in Figure S7). The coated cellulose capillary was in general necessary for the analysis of LONs with the noticeable exception of **k-LON<sup>G4</sup>**. Unless the LON forms stable micellar assemblies as in the case of **k-LON<sup>G4</sup>**, unspecific adsorption was observed onto the uncoated capillary with the other LONs as evidenced by a trailing in the absorption curve of the chromatogram.

**TEM** analyses were performed at the Bordeaux Imaging Center (BIC) of the University of Bordeaux using an Hitachi H7650 at a voltage of 80kV. For sample preparation a drop of 100 nM solution of 1-LON<sup>G4</sup>, 2X selex salts was placed on a carbon film 200 Mesh copper grid and left to dry for 10 min. A drop of 1% uranyl acetate solution as a negative stain for 1 min was then added to the copper grid and left to dry.

**NMR** analysis were performed at the Institut Européen de Chimie Biologie (IECB) using a 700MHz NMR Bruker spectrometer. Samples concentrations were 100 $\mu$ M. Experiments were performed at 25°.

**Figure S1. General structures of the different Lipid OligoNucleotides (LONs) synthesized**



NAME	Lipid =	Lipidic phosphoramidite
<b>ON</b>	None (5'-OH)	None
<b>1-LON<sup>G4</sup></b>	<i>n</i> -C <sub>18</sub> H <sub>37</sub>	
<b>k-LON<sup>G4</sup></b>	ketal bis-C <sub>15</sub>	

5'- TTA GT **T GGG GT T** CAG TTG G -3' : **ON<sup>G4</sup>**  
 5'- TGT AGT AGG TTG TGT CTG G -3' : **ON<sup>SC</sup>**  
***n*-C<sub>18</sub>H<sub>37</sub>** -5'- TTA GT **T GGG GT T** CAG TTG G -3' : **1-LON<sup>G4</sup>**  
***n*-C<sub>18</sub>H<sub>37</sub>** -5'- TGT AGT AGG TTG TGT CTG G -3' : **1-LON<sup>SC</sup>**  
**ketal**-5'- TTA GT **T GGG GT T** CAG TTG G -3' : **k-LON<sup>G4</sup>**  
**ketal**-5'- TGT AGT AGG TTG TGT CTG G -3' : **k-LON<sup>SC</sup>**

The ON<sup>G4</sup> was reported to bind to the ampicillin antibiotic<sup>1</sup>.

**T GGG GT** corresponds to the G4-prone forming sequence.

General salt conditions = **1X** = 50mM NaCl, 5mM KCl, 5mM MgCl<sub>2</sub>

**2X, 3X** etc. refer to the salt being concentrated 2, 3, etc. times.

<sup>1</sup> K.-M. Song, E. Jeong, W. Jeon, M. Cho and C. Ban, *Anal. Bioanal. Chem.*, 2012, **402**, 2153–2161.

**MALDI-TOF mass analyses:**

**1-LON<sup>G4</sup>**: [M+H]<sup>+</sup> calculated MW: 6254.28 Da, found: 6257.42 Da (0.050% error);

**1-LON<sup>SC</sup>**: [M+H]<sup>+</sup> calculated MW: 6254.28 Da, found: 6256.69 Da (0.039% error).

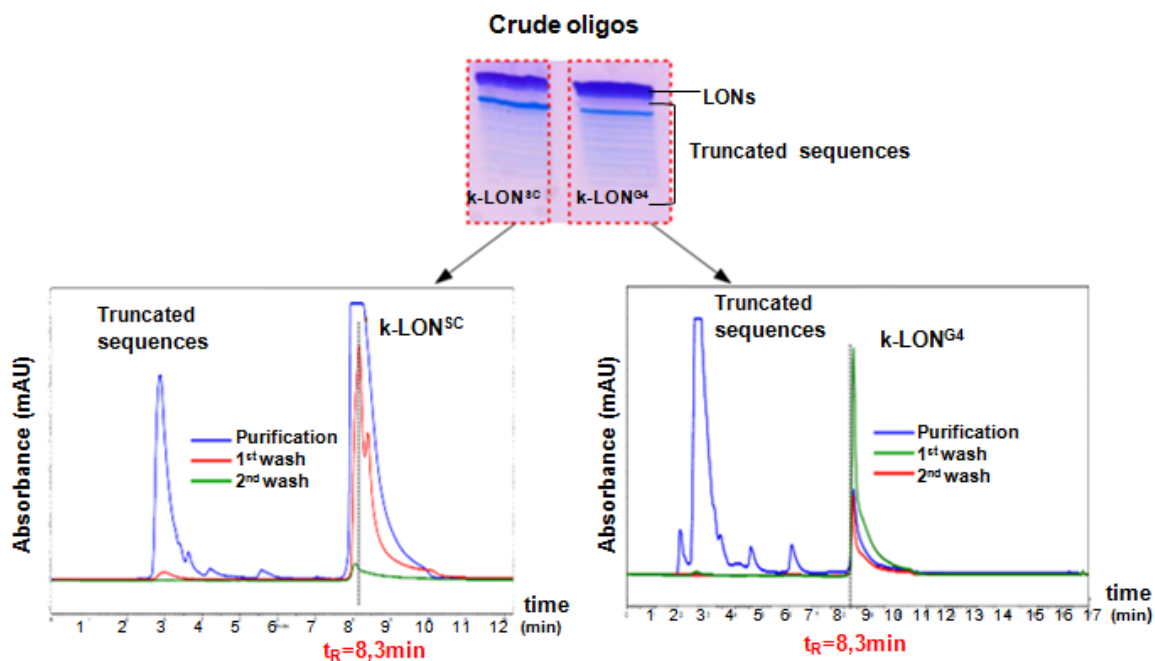
**k-LON<sup>G4</sup>**: [M+H]<sup>+</sup> calculated MW: 6660.80 Da, found: 6660.2 Da (0.009% error);

**k-LON<sup>SC</sup>**: [M+H]<sup>+</sup> calculated MW: 6660.80 Da, found: 6662.6 Da (0.027% error).

**ON<sup>G4</sup>**: [M+H]<sup>+</sup> calculated MW: 5921.90 Da, found: 5924.29 Da (0.039% error).

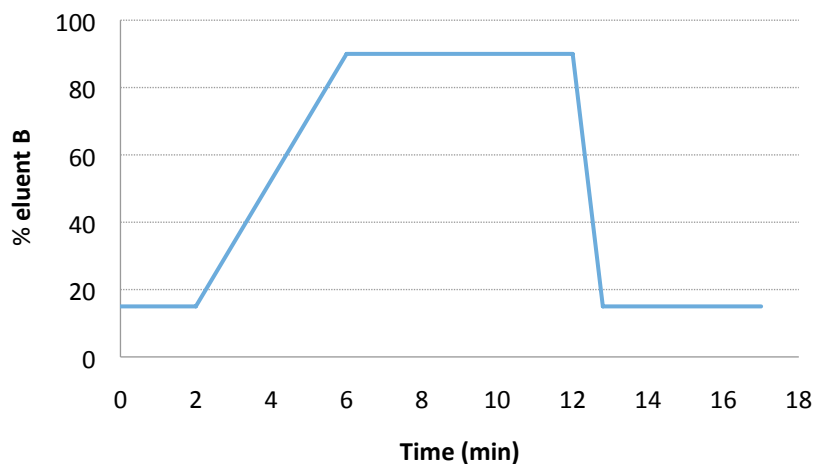
**ON<sup>SC</sup>**: [M+H]<sup>+</sup> calculated MW: 5921.90 Da, found: 5924.22 Da (0.040% error).

Figure S2. Crude oligo PAGE profiles of k-LON<sup>SC</sup> and k-LON<sup>G4</sup> and their corresponding RP-HPLC purification chromatograms.



Top: Similar denaturing PAGE profiles for the crude k-LON<sup>G4</sup> and k-LON<sup>SC</sup> after automated chemical synthesis (before purification): both LONs are expected to be present in roughly the same proportions in the crude in HPLC. Bottom: HPLC purification of the corresponding crudes (the Y axis corresponds to the absorbance recorded at 260nm in normalized arbitrary units).

RP-HPLC conditions: C<sub>4</sub> semi preparative column (Macherey Nagel, Nucleosil, 5µm, 250mm), flow rate 5 mL/min mobile phase eluent A: 0.1M triethylammonium acetate pH 7.1 / CH<sub>3</sub>CN (95/5, V/V), eluent B : 0.1M triethylammonium acetate pH 7.1 / CH<sub>3</sub>CN (20/80, V/V).



Method diagram. Start at 15% B, increase to 90% B, then decrease to 15% B. Total method time 17min.

While the scramble **k-LON<sup>SC</sup>** was readily purified by reverse phase (C<sub>4</sub>) HPLC (left, retention time = 8.3 min)), very little quantities of **k-LON<sup>G4</sup>** was obtained after the first injection of the crude mixture (blue profile on the right, same retention time). More **k-LON<sup>G4</sup>** (but still little quantities) was collected after the injection of a pure water sample (green profile). The very stable micelles of **k-LON<sup>SC</sup>** most probably were retained on the column and a very small fraction of monomers eluted after the injection of water as a result of the absence of salts in the water.

Figure S3. Experimental setup for the electro-elution of **k-LON<sup>G4</sup>** from preparative polyacrylamide gel.

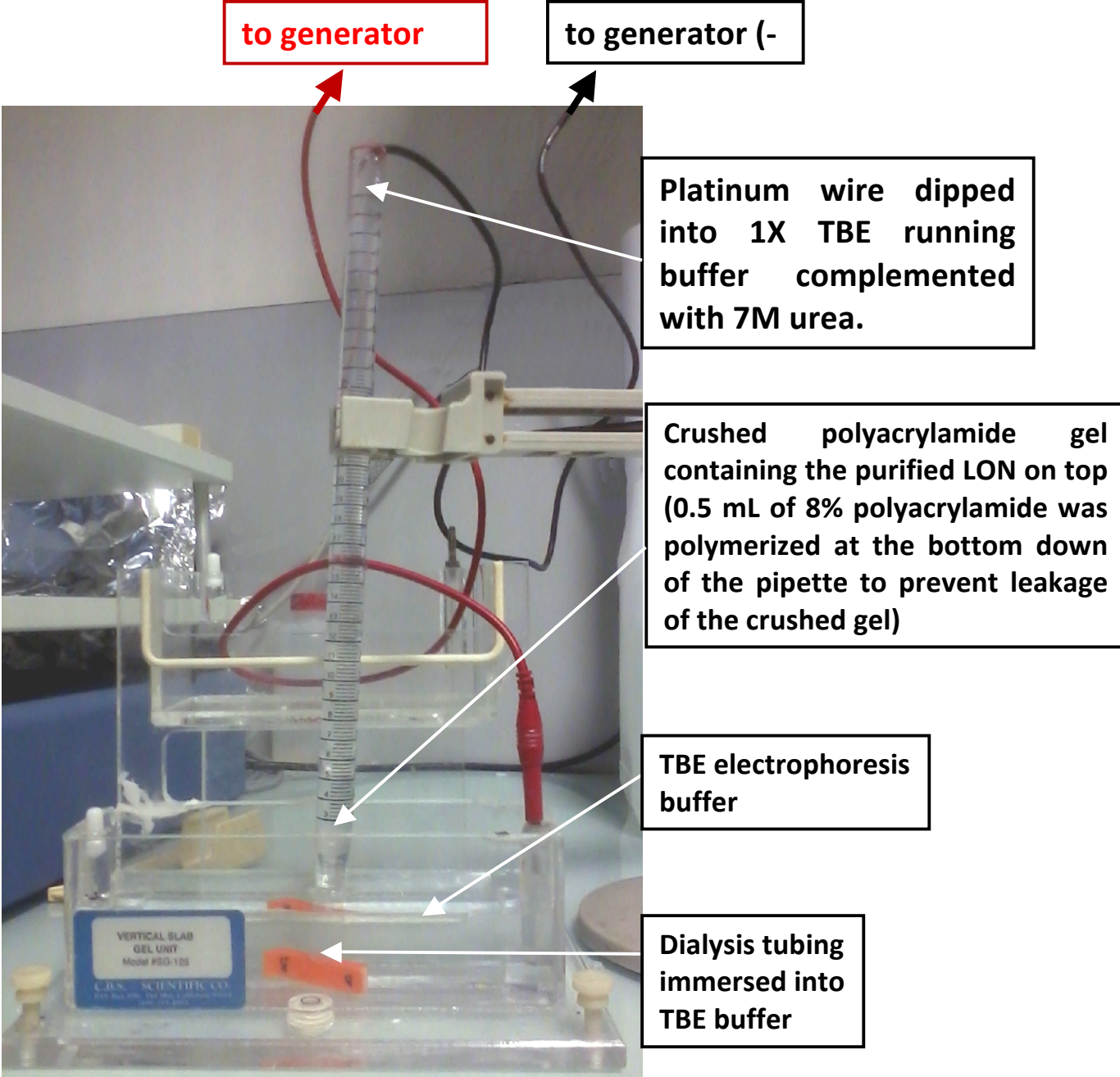
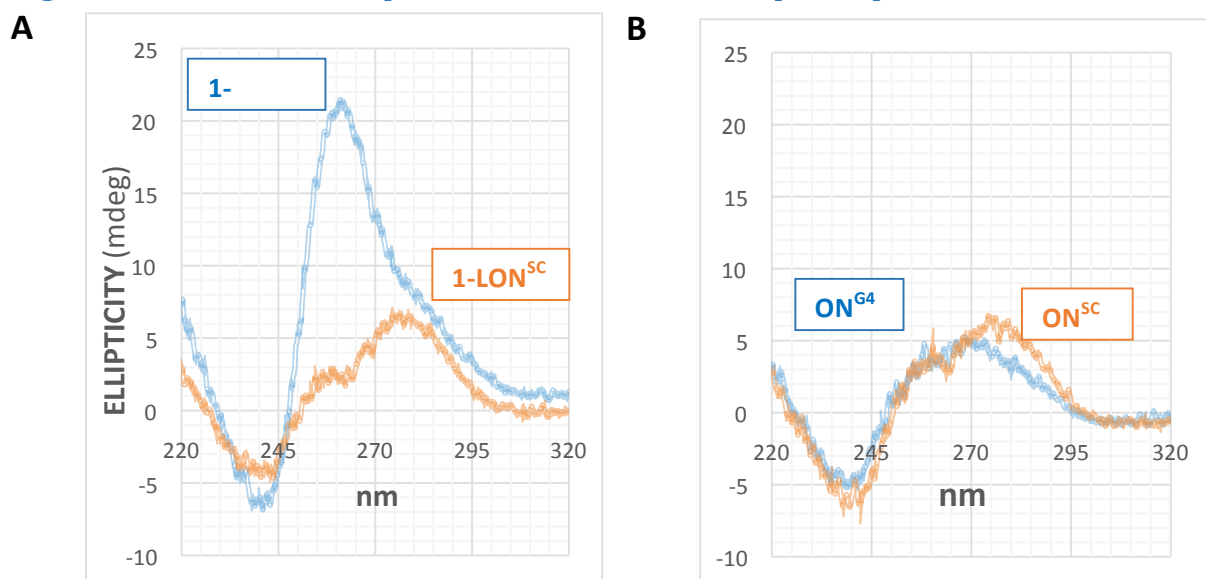
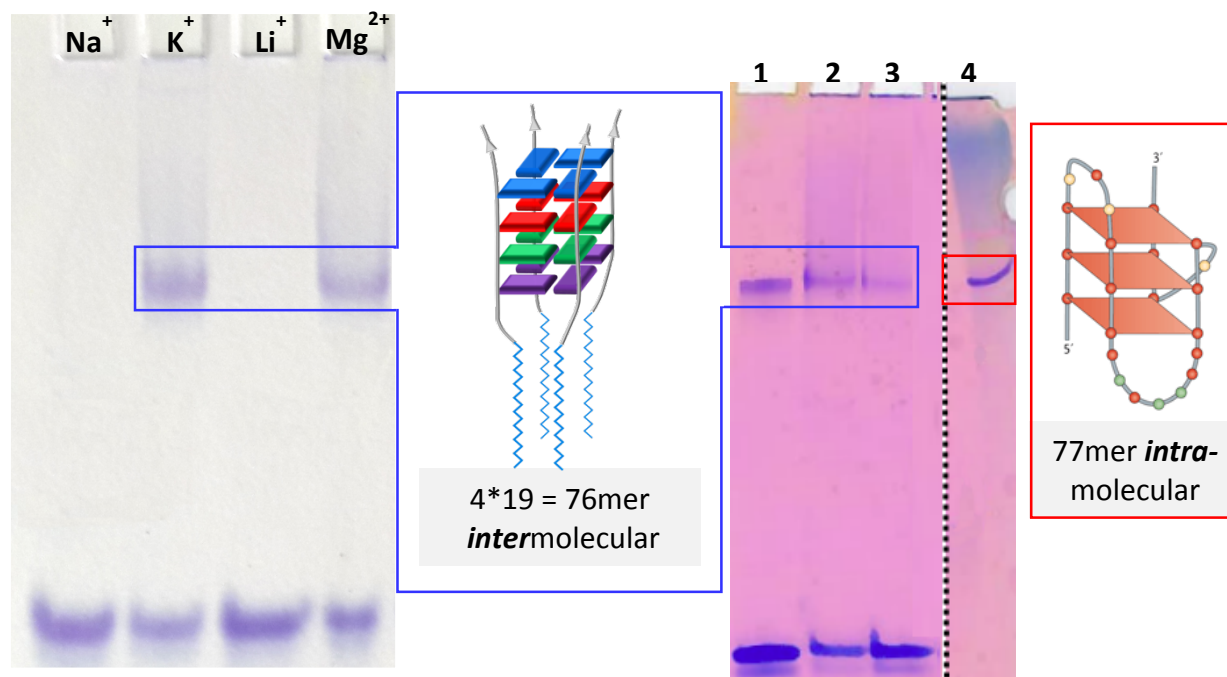


Figure S4. Evidence for a parallel tetramolecular G-quadruplex with **1-LON<sup>G4</sup>**.



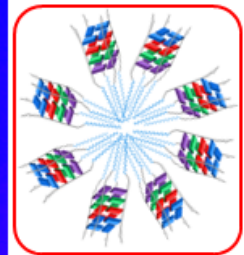
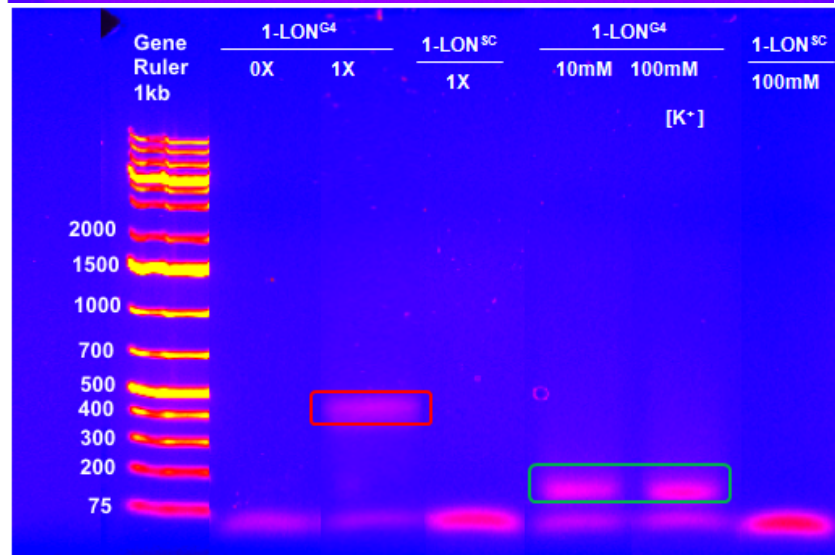
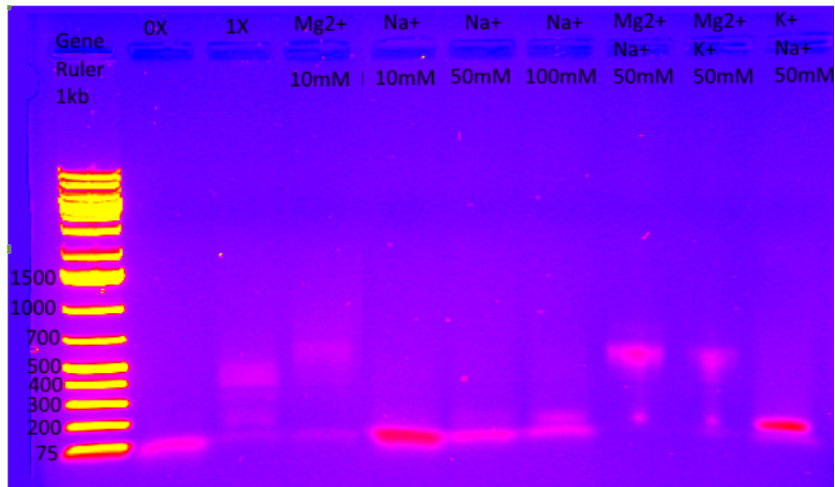
Conditions: [LON] = 5 $\mu$ M (diluted from original 30 $\mu$ M solutions), **1X** salts, phosphate buffer pH 6.9 20mM.

**C**



- 1:** no salts
- 2:** 1X: 50mM NaCl, 5mM KCl, 5mM MgCl<sub>2</sub>
- 3:** 55mM LiCl, 5mM MgCl<sub>2</sub>
- 4:** control intramolecular 77-mer G4

D



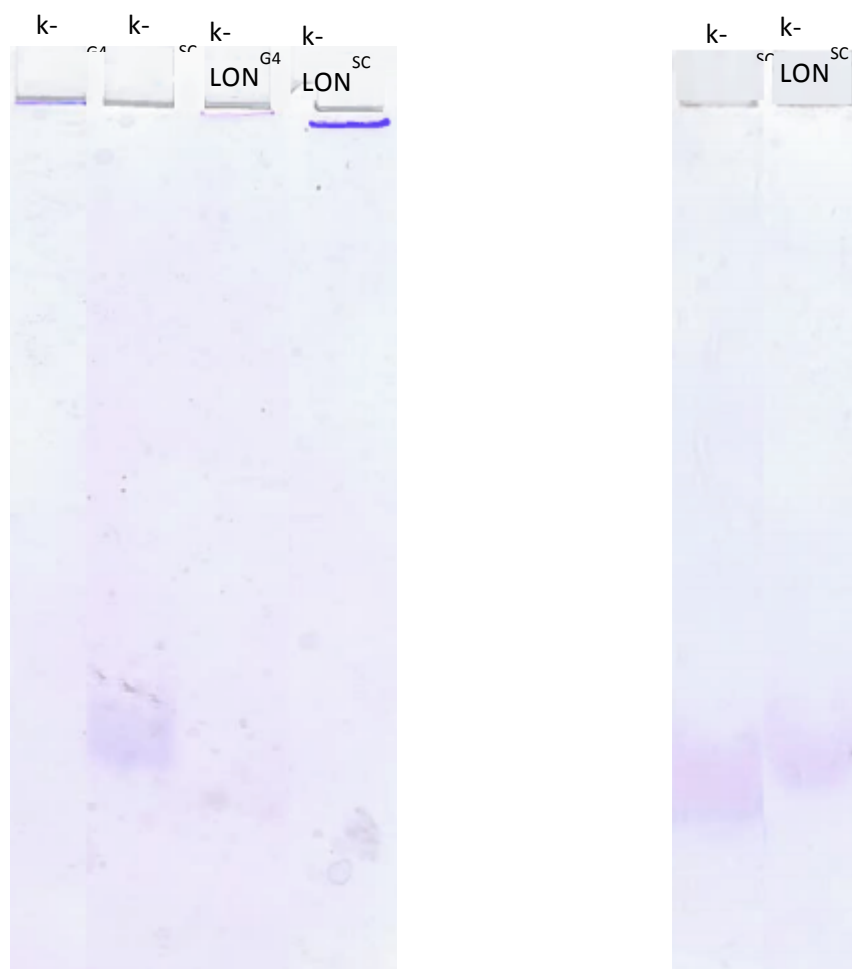
E

**A:** While the scramble sequence **1-LON<sup>SC</sup>** does not show any noticeable folding, **1-LON<sup>G4</sup>** exhibit the CD profile observed for parallel G-quadruplexes (RM: no temperature gradient cycles have been used here). **B:** in line with PAGE results, the unmodified **ON<sup>G4</sup>** do not give any CD G4-signature. **C:** Native PAGE of **1-LON<sup>G4</sup>** in different salts conditions (left, 100mM salts) and with a 77-mer intramolecular G-quadruplexe structure (lane 4) as a control (right). The band for the intramolecular G4 (77-mer) migrated similarly as the retarded tpG4 band from **1-LON<sup>G4</sup>** (4\*19-mer). The trailing of the retarded band in the gel is due to the absence of EDTA in the gel. In fact, the trailing is more visible when Mg<sup>2+</sup> is present in the deposit and results from the partial disruption of **1-LON<sup>G4</sup>** micellar aggregates as can be seen by the absence of trailing in the absence of added salts (lane 1). **D:** Salt-dependency for the stabilization of **1-LON<sup>G4</sup>** micellar aggregates. While no micelles are visible in the absence of salt (0X lanes), micelles are only visible in the presence of Mg<sup>2+</sup> (1X lane). Interestingly, only **1-LON<sup>G4</sup>** tpG4 are visible in the presence of only K<sup>+</sup>. Micelles are nevertheless present in solution under these conditions (DLS data not shown), they are not stable enough to survive the electrophoresis conditions.

Figure S5. Partitioning or lack of partitioning for **k-LON<sup>SC</sup>** and **k-LON<sup>G4</sup>** monomers respectively into triton or SDS micelles.

With or w/o 17mM Triton (>cmc)

same conditions with 23 mM SDS (>cmc)



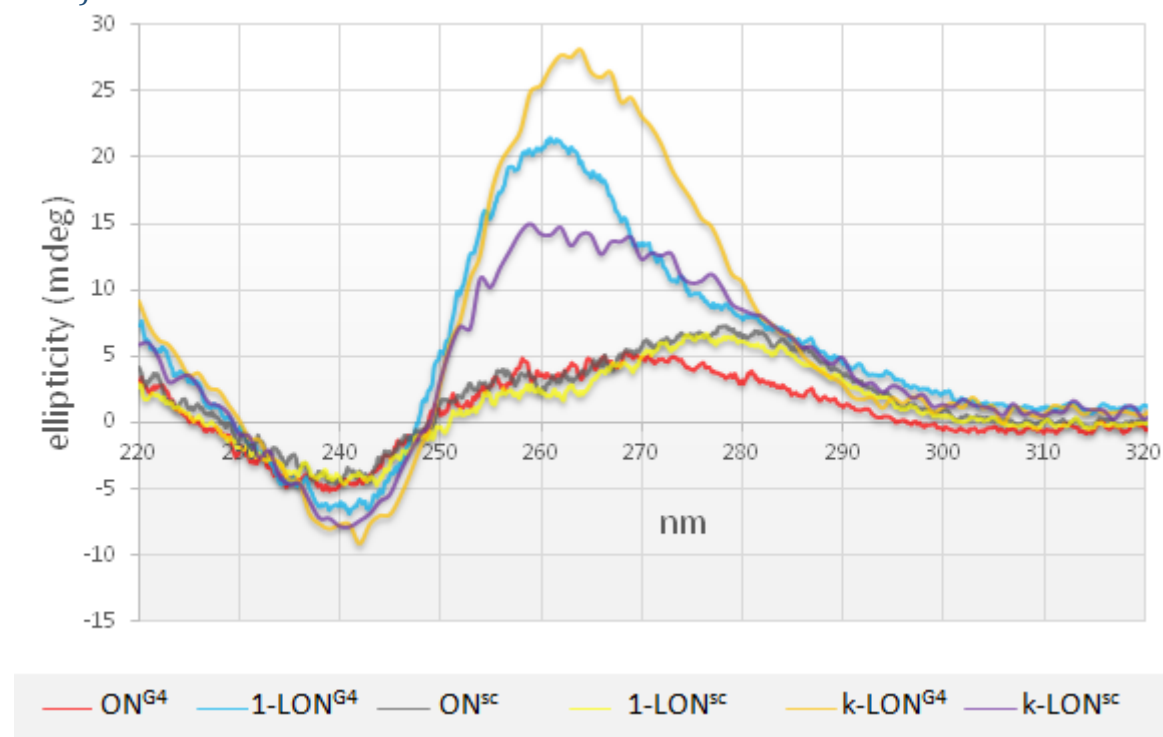
Conditions: [LON] = 16 $\mu$ M, **1X** salts, TB buffer 0.5X, U=50V limiting for the electrophoresis.

The LONs were denatured at 95°C in the presence of the salts. The detergent was added thereafter while the sample was still warm and the mixture was left renaturing at 20°C for 8h before electrophoresis.

RM: the trailing of the bands results from the absence of EDTA in the running buffer.

Figure S6. G4 signature for **k-LON<sup>G4</sup>**.

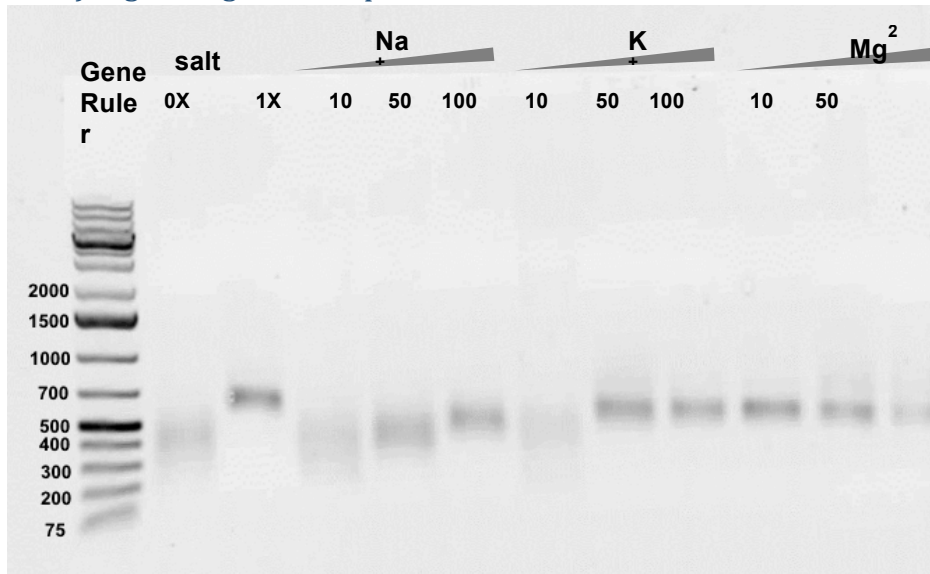
A) Circular Dichroism:



Conditions:  $[\text{LON}] = 5\mu\text{M}$  (diluted from original  $30\mu\text{M}$  solutions), **1X** salts, phosphate buffer pH 6.9 20mM.

In line with PAGE results under low salts conditions, the G4 structure was not detected for the unmodified  $\text{ON}^{\text{G4}}$ . Both  $\text{k-LON}^{\text{G4}}$  and  $1\text{-LON}^{\text{G4}}$  CD signatures are in agreement with a parallel G4 folding. Interestingly,  $\text{k-LON}^{\text{SC}}$  showed a tendency to form G4 structures too. The micellisation of the LON leads to a high local concentration of G-rich DNA sequences that may be in part responsible for the formation of these G-quadruplexes.

B) Agarose gel electrophoresis:

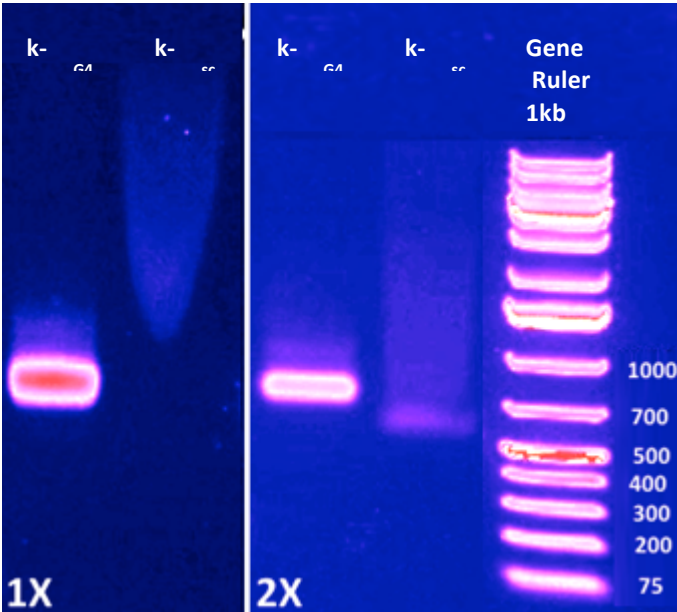


Conditions: [k-LON<sup>G4</sup>] = 30μM in different salt conditions, in 20mM phosphate buffer pH 6.9. Agarose gel 1%, TB buffer 0.5X, 100V for the electrophoresis. (0X corresponds to the absence of added salts, the concentrations are expressed in mM).

1X salts: 50mM NaCl, 5mM KCl, 5mM MgCl<sub>2</sub>

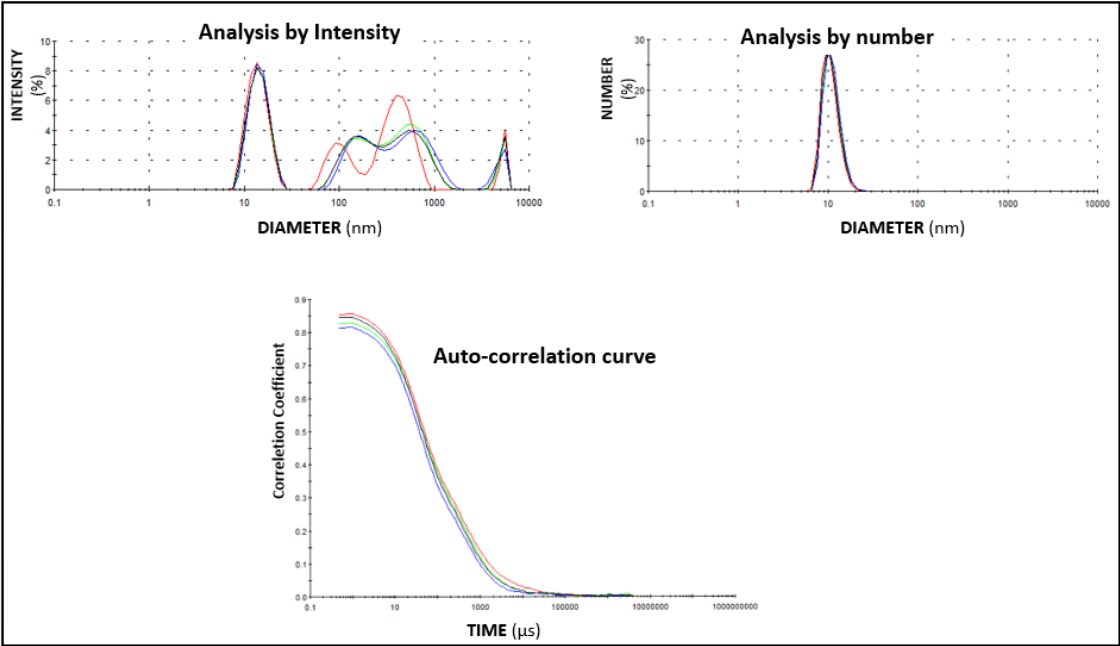
Compared to Na<sup>+</sup>, K<sup>+</sup> is a more potent stabilizer of the micellar aggregates from k-LON<sup>G4</sup> as judged by the sharper and more retarded micellar bands obtained at 50mM salt concentrations.

Figure S7. Agarose gel (1%) and DLS experiments with **k-LON<sup>SC</sup>**.



Conditions: [LON] = 20 $\mu$ M, **1X** salts (left) and **2X** (right), TB buffer 0.5X.

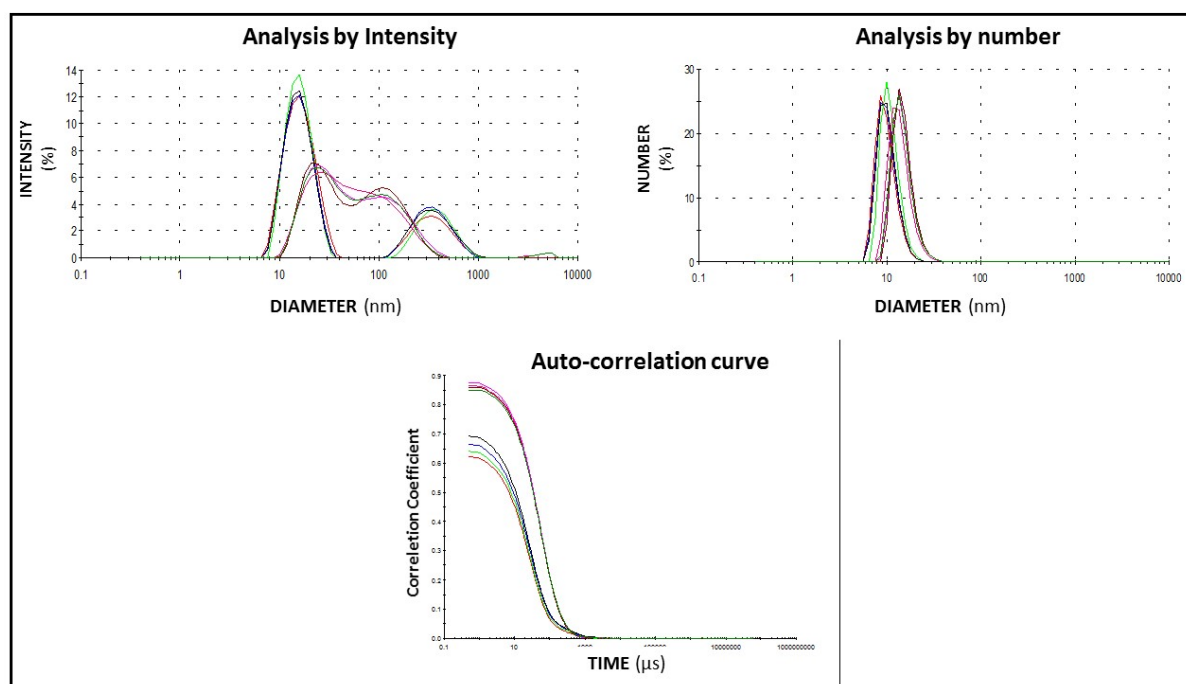
Trailing of the **k-LON<sup>SC</sup>** band is clearly visible in the presence of 1X salts (left). When the salt concentration is doubled (right), the monomer band appears. The trailing of the bands with **k-LON<sup>SC</sup>** most likely results from unspecific interactions between the scramble oligonucleotides and the agarose gel matrix (see below).



Superimposition of 4 consecutive **k-LON<sup>SC</sup>** DLS profiles of a 50 $\mu$ M solution in PBS buffer 10mM, **1X** salts. Results analyzed in intensity mode (top left), number (top right) and the original auto-correlation function.

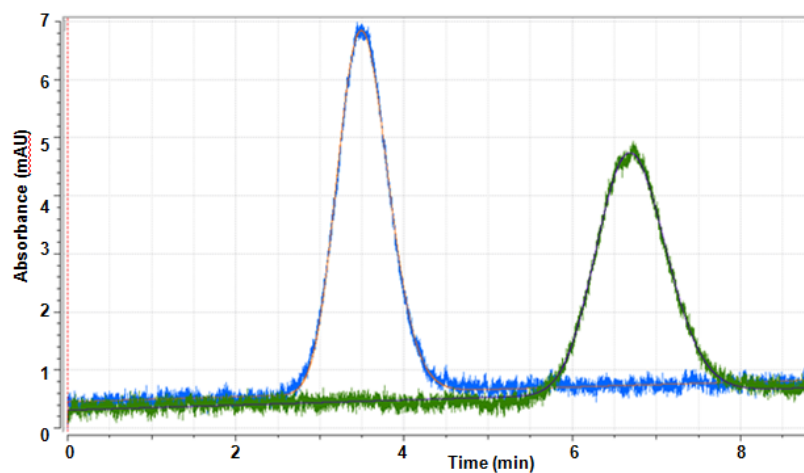
DLS and TDA analysis (not shown) clearly ruled out the putative presence of large aggregates for **k-LON<sup>SC</sup>** in solution. Even in the very large particles-sensitive intensity mode does no or very few large aggregates detected (top left). Instead, micelles that are formed from **k-LON<sup>SC</sup>** present a large local concentration of unstructured DNA that may interact in an unspecific manner with the agarose gel matrix. Smith et al. (*Anal. Biochem.* **1983**, *128*, 138- 151) reported this phenomenon and noticed that the trailing was more pronounced as DNA molecular weight was increased and salt concentration was decreased. In line with our observations, the trailing of **k-LON<sup>SC</sup>** micelles was less severe when the salt concentration was doubled (see 1X vs 2X salts agarose gels above).

DLS profiles of **k-LON<sup>G4</sup>** and **k-LON<sup>SC</sup>** micelles.

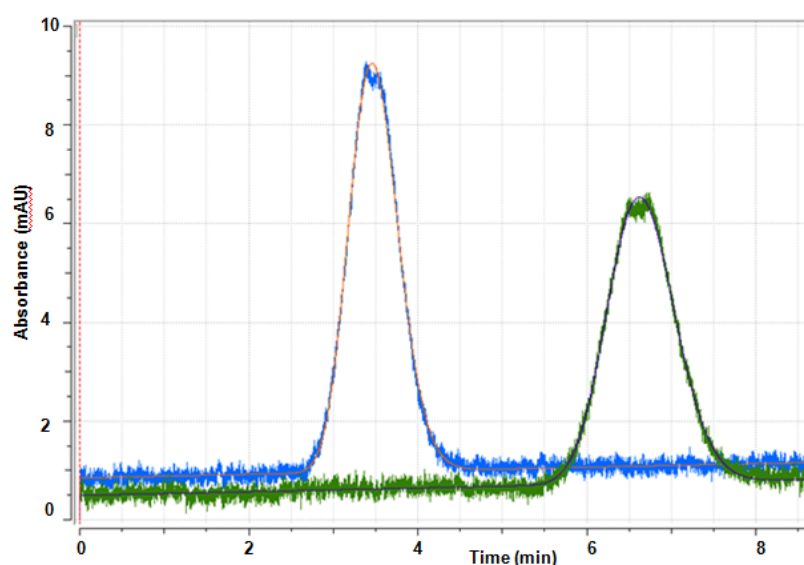


Conditions: [LON] = 30 $\mu$ M, **1X** salts, phosphate buffer pH 6.9 20mM.

Figure S8. TDA of **k-LON<sup>G4</sup>** and **k-LON<sup>SC</sup>** micellar sizes.



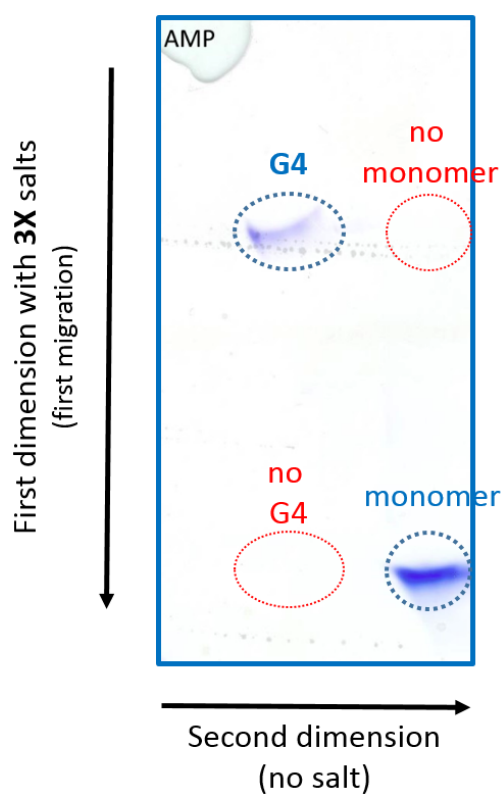
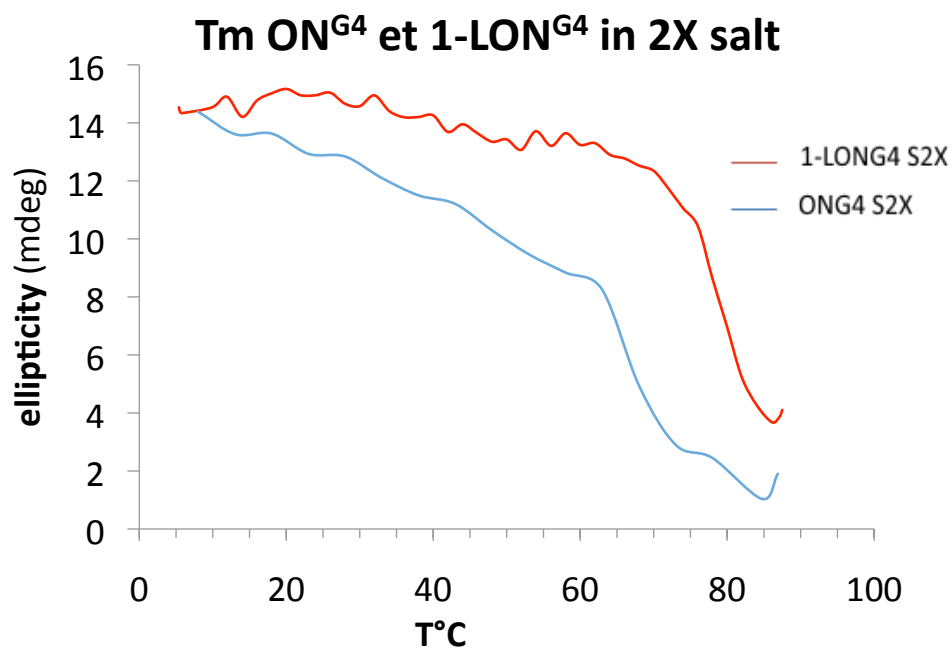
**k-LON<sup>G4</sup>** :  $\lambda=254\text{nm}$ ; hydrodynamic radius 6,216 nm; diffusion coefficient  $39,5 \mu\text{m}^2/\text{s}$ .



**k-LON<sup>SC</sup>** :  $\lambda=254\text{nm}$ ; hydrodynamic radius 5,787nm; diffusion coefficient  $42,4 \mu\text{m}^2/\text{s}$ .

TDA of 30 $\mu\text{M}$  solutions of **k-LON<sup>G4</sup>** (top) and **k-LON<sup>SC</sup>** (bottom) in 3X salts in PBS buffer 10mM pH 6.9. The blue curve corresponds to the absorption signal in the first analysis window, the green one in the second window. The red and violet lines correspond to the fitting curve from which the hydrodynamic radius is extracted.

Figure S9. Stability of 1-LON<sup>G4</sup> tpG4.



Conditions: [ON<sup>G4</sup>] = 60μM, TBE buffer 0.5X.

The ON<sup>G4</sup> aptamer was deposited concentrated and in the presence of 3X salts to favor the formation of G4 quadruplexes. After the first migration was stopped, the oligonucleotides were left equilibrating for 2h after which the second electrophoresis was carried out in the second dimension (90° relative to the first one). The second migration therefore took place with no salt added. The

absence of added salts that promote the formation of the G4 structures and the dilution of the sample in the gel may explain the absence of G4 in the second migration of the monomer band (bottom left, circled in red). This experiment clearly demonstrates that once formed, the tpG4 is inert as no monomer band is observed in the second dimension of the G4 band (top right in red). It is worth emphasizing that the G4 remained stable for 2h despite the absence of stabilizing salts in the gel during the course of the second migration.

Figure S10. Effect of temperature cycles for 1-LON<sup>G4</sup>.

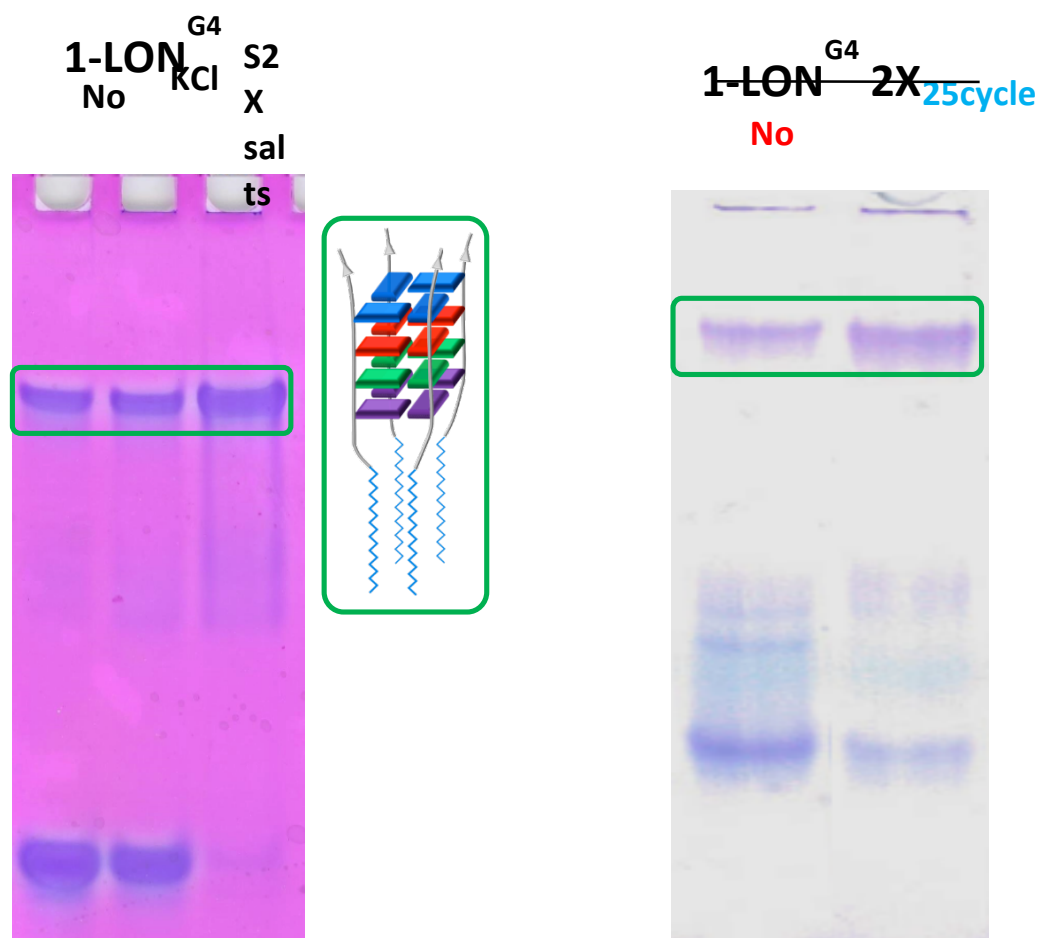
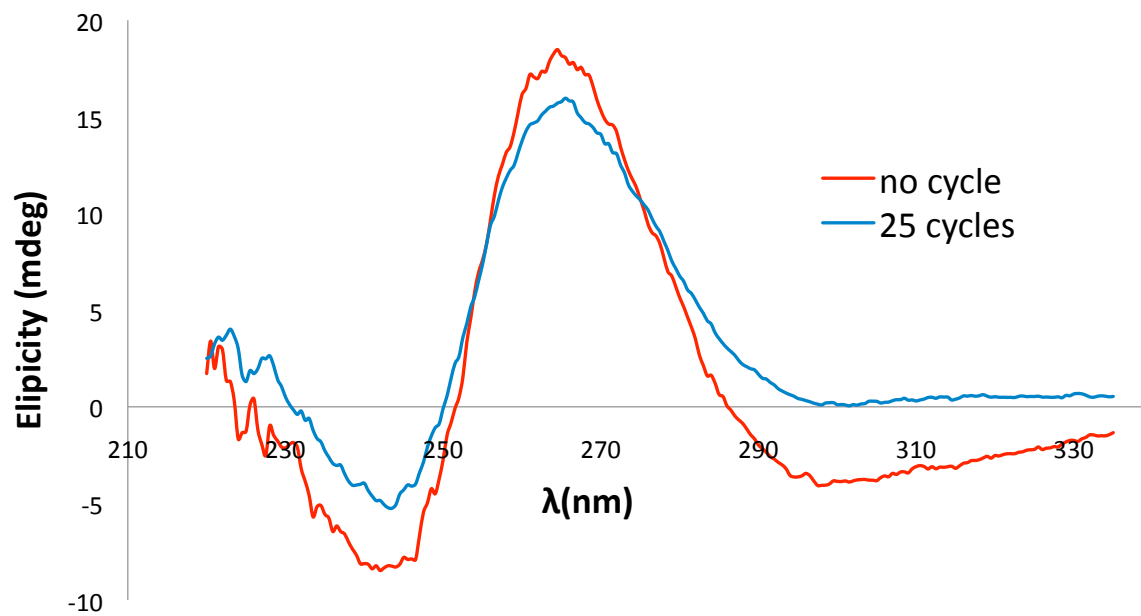


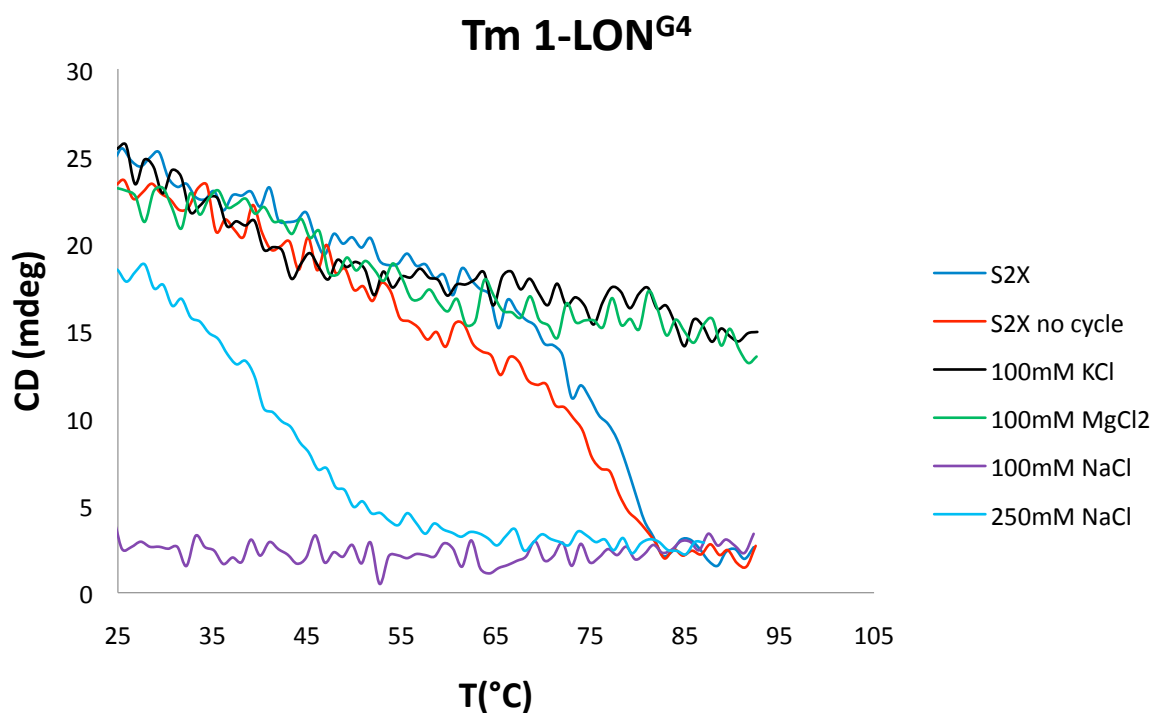
Figure S11. Effect of temperature cycles for **1-LONG<sup>G4</sup>**.



CD spectra of 1-LONG4 without (red) and with temperature cycles (25 cycles, blue) of a 5  $\mu$ M solution in the presence of 2X salts and 20mM phosphate buffer.

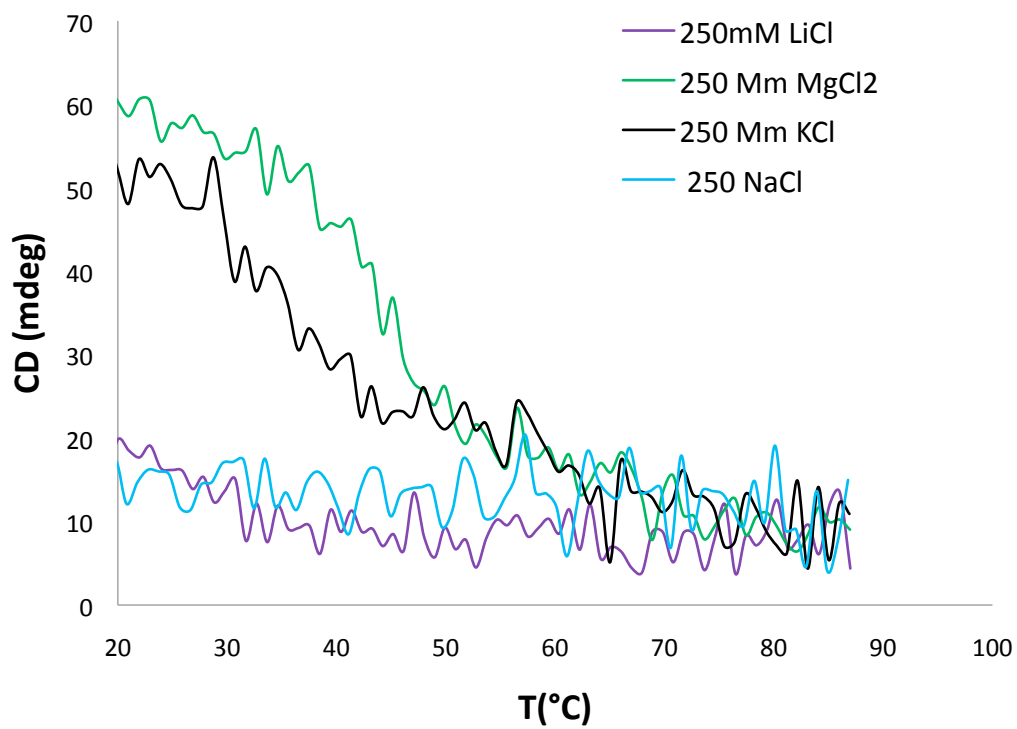
Figure S12. Effect of cations on the thermal stability of **1-LON<sup>G4</sup>** and **ON<sup>G4</sup>** tpG4s.

### 1-LON<sup>G4</sup>



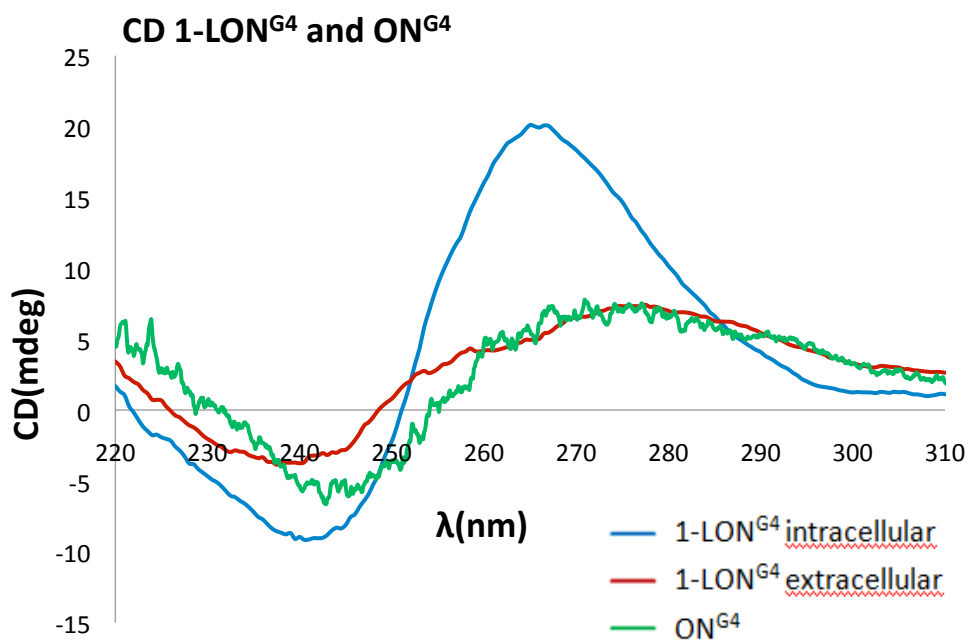
CD Melting curves of **1-LON<sup>G4</sup>** in the presence of different cations (5 $\mu$ M LON solutions in phosphate buffer 20mM).

No melting is observed in the presence of 100mM magnesium (green) or potassium (dark grey): T<sub>m</sub> > 95°C. In contrast, the T<sub>m</sub> is very low < 20°C in the same conditions with sodium. We had to increase the sodium concentration to 250mM to observe the transition (light blue curve). Sodium is clearly a competitor for tpG4 binding as the T<sub>m</sub> is decreased in the presence of a mixture of the 3 salts (red and blue curves, same conditions the latter with additional temperature cycles applied).

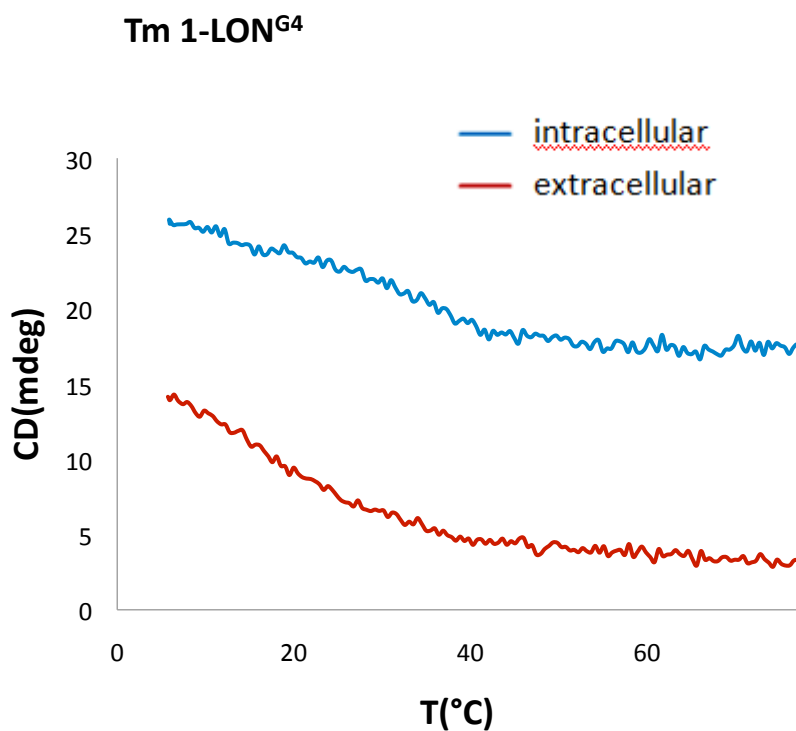


Same experiments with **ON<sup>G4</sup>**. The same behavior is observed.

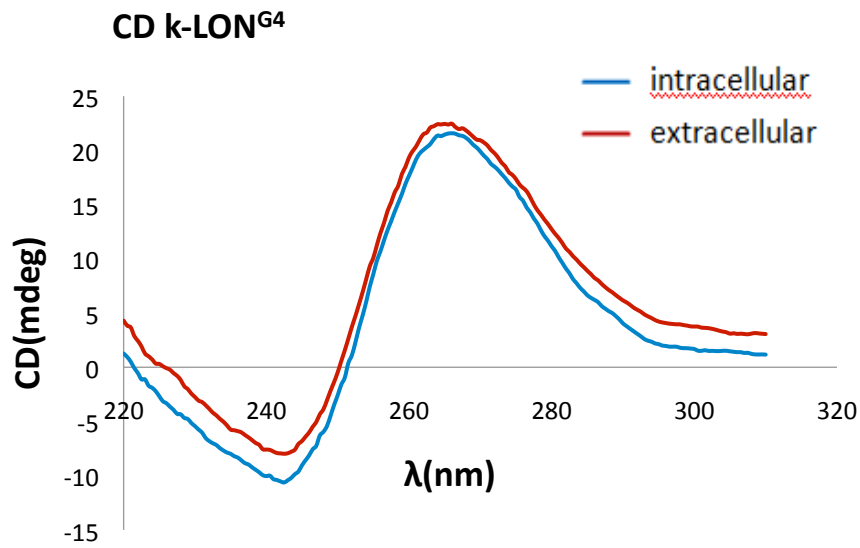
Figure S13: Effects of cations at intra and extracellular concentrations on the thermal stability of 1-LON<sup>G4</sup> and k-LON<sup>G4</sup>



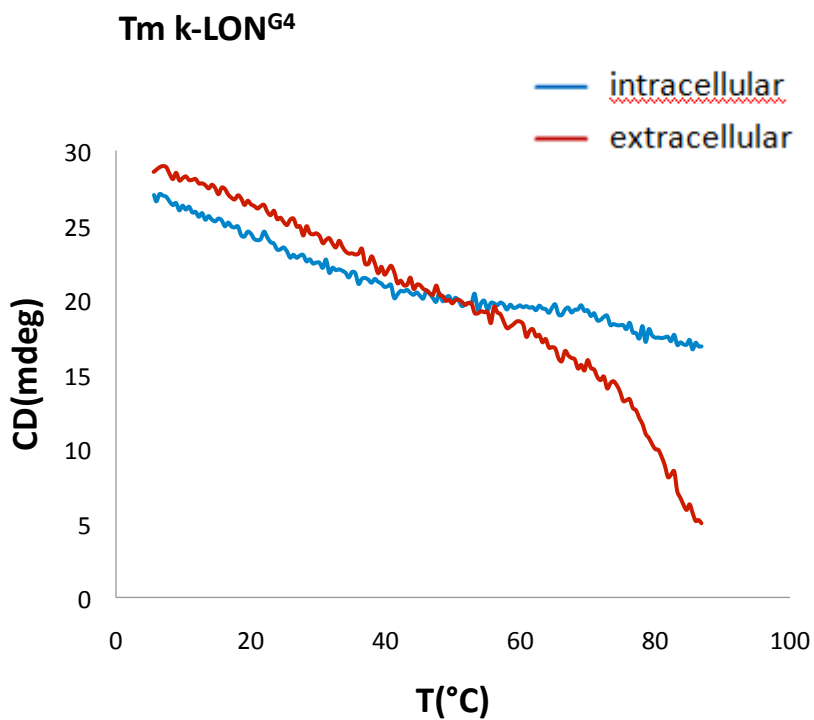
CD spectra of **1-LON<sup>G4</sup>** at intracellular (blue, 140mM KCl, 12mM NaCl, and 1mM MgCl<sub>2</sub> ) and extracellular (red, 5mM KCl and 145mM NaCl) salt concentrations at 37°C. Under extracellular salt conditions **1-LON<sup>G4</sup>** is not folded just as the control **ON<sup>G4</sup>** (green, see main text for details).



CD melting curve of **1-LON<sup>G4</sup>** extracted at 265nm at intracellular cation concentrations (blue) and extracellular concentrations (red).



CD spectra of **k-LON<sup>G4</sup>** at 37°C of intracellular (blue) and extracellular (red) concentrations.



CD melting curve extracted at 265nm of **1-LON<sup>G4</sup>** at intracellular (blue) and extracellular (red) concentrations: the perfect tetramolecular parallel G4 melts only at extracellular salt concentrations. The steady decrease observed at low temperatures correspond to the melting of mismatch parallel G4s.

